Macromolecular Research

Article

DOI 10.1007/s13233-020-9094-0 www.springer.com/13233 pISSN 1598-5032 eISSN 2092-7673

Dual-Responsive Cross-Linked Micelles from Amphiphilic Four-Arm Star Copolymers with Different Block Ratios for Triggering DOX Release

Yunwei Huang[1]
Yanzhe Li[1]
Zilun Tang[1]
Qiuping Su[1]
Tingting Liao[1]
Yuxin Gu[2]
Xiaofeng Lin[1]
Xihong Zu[1]
Wenjing Lin*[,1]
Guobin Yi*[,1]

[1] School of Chemical Engineering and Light Industry, Guangdong University of Technology, Guangzhou 510006, P. R. China
[2] Guangdong Provincial Key Laboratory of Advanced Coatings Research and Development, Guangzhou Kinte Industrial Co., Ltd., Guangzhou 510300, P. R. China

Received January 5, 2020 / Revised February 10, 2020 / Accepted February 14, 2020

Abstract: The four-arm star copolymers poly(methacrylic acid)-poly(2-hydroxyethyl methacrylate-disulfide~)-poly(poly(ethylene glycol) methyl ether methacrylate) (4AS-PMAA$_x$-(PHEMA-SS~)$_y$-PPEGMA$_z$) with four different block ratios were synthesized and could self-assembled into cross-linked polymer micelles for the exploration of the structure-property relationship. The cross-linked polymer micelles in aqueous solution had low critical micelle concentration (CMC) values (1.9-4.6 mg/L), which exhibited better stability than non-cross-linked micelles. The CMC value decreased with the increase of the length of inner PMAA core and hydrophobic PHEMA cross-linked middle layer. The blank and doxorubicin (DOX)-loaded micelles with different block ratios were prepared by dialysis with the particle sizes of 120-240 nm. The longer inner PMAA core and cross-linked middle layer enhanced the drug loading content (DLC) results and led to relatively bigger particle sizes of polymer micelles. The *in vitro* DOX release data revealed that DOX-loaded micelles had low DOX cumulative release percentages of 18-37% after 110 h at pH 7.4, but up to 83-90% when introducing reductant GSH at pH 5.0. The 4AS-PMAA$_{21.2}$-(PHEMA-SS~)$_{13.1}$-PPEGMA$_{5.1}$ micelles with the longest PMAA core had the largest cumulative release of 90.1%. The DOX release process and mechanism of the micelles at different conditions fitted well with the semi-empirical equation. Overall, the results demonstrated that the block ratios and pH/redox-responsiveness of these four-arm star copolymers could be well-controlled and their self-assembled cross-linked micelles as anticancer drug carrier system could be improved by optimizing the different ratios.

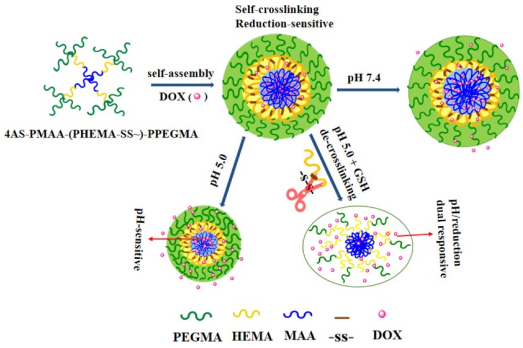

Keywords: dual-responsive, cross-linked micelles, cancer, drug release kinetics.

1. Introduction

In recent decades, polymer micelles have been widely used as nanocarriers in antitumor drug delivery systems.[1-5] Polymer micelle is a kind of nanoparticle self-assembled by amphiphilic copolymer in aqueous solution, and the hydrophobic anticancer drug can be packaged into the hydrophobic core of micelle while the hydrophilic shell can improve the stability of micelle to prolong circulation duration in the body. Among various polymer micelles, cross-linked micelles self-assembled from star-shaped polymers have attracted extensive attention.[6-9] Star-shaped polymer is formed by three or more branched chains from the same central core, and the micelles formed by star polymers have better stability than those of formed by linear polymers. The cross-linked micelles formed by star-shaped polymers have stable chemical structures to prevent the decomposition of micelles by the dilution and chemical environment change in circulating, and the cross-linked structure within a large number of cavities can also improve the micellar drug loading to enhance the anticancer efficiency.

The anticancer drug delivery system is a kind of intelligent delivery system, which can response to endogenous stimuli (pH, redox, *etc.*) and exogenous stimuli (temperature, magnetic, electric field, enzyme, light, *etc.*) with corresponding physical or chemical changes to release drug.[10-16] To achieve drug release efficiently under stimulated condition, polymer micelles should introduce specific chemical structures to meet the stimulus-responsive

Acknowledgments: The authors gratefully acknowledge the financial support from the National Natural Science Foundation of China (No. 51873042, No. 21808039), the Natural Science Foundation of Guangdong Province (No. 2018A030310525), the Science and Technology Planning Project of Guangdong Province (No. 2017B090915004), and the Guangdong Provincial Key Laboratory of Advanced Coatings Research and Development (No. 2017B030314105).

***Corresponding Authors:** Wenjing Lin (Wenjing.Lin@gdut.edu.cn), Guobin Yi (yigb@gdut.edu.cn)

properties. However, the more stimulus-responsiveness introduces, the more complex micellar structure will be inevitably caused. Therefore, at present, most studies are still focused on dual-stimuli-responsive drug delivery system.[17-19] Sang *et al.* obtained pH and reduction dual-responsive polymeric micelles for the anticancer drug delivery. After loading the anticancer drug DOX, the micelles exhibited accelerated drug release behaviors in acidic and GSH-triggered tumor sites while inhibited premature release behaviors in normal tissue conditions.[20]

The optimization of polymer structure for improving the efficacy of micelles as drug carrier system while developing new polymers is a hot research topic at present stage.[21,22] Zhang *et al.* studied the effect of the hydrophilic/hydrophobic ratio of polymeric micelles, and found that the ratio was an important parameter in design and engineering of drug vehicles for cancer therapy.[23] Yang *et al.* prepared a series of amphiphilic triblock polymer micelles for controlled anticancer drug delivery, and discovered that the drug release was closely related to the hydrophilic/hydrophobic ratio of the micelles.[24] However, limited work on the relationships between the hydrophilic/hydrophobic ratios and dual-stimuli-responsive cross-linked micelles physicochemical properties of the star polymers has been reported. Some dual-sensitive cross-linked micelles have still not reached satisfied performances. Thus, the exploiting of hydrophilic/hydrophobic ratios-properties relationships and construction of novel dual-sensitive polymers with suitable structure would be a fascinating way to improve the nanoplatform performances.

Based on that, in this current work, four kinds of star-shaped amphiphilic copolymers poly(methacrylic acid)-poly(2-hydroxyethyl methacrylate-disulfide~)-poly(poly(ethylene glycol) methyl ether methacrylate) (4AS-PMAA$_x$-(PHEMA-SS~)$_y$-PPEGMA$_z$) with the same blocks and different block ratios were synthesized by activators regenerated by electron transfer atom transfer radical polymerization (ARGET ATRP) following with Michael addition reaction and hydrolysis, and then self-assembled into three layers cross-linked polymer micelles in aqueous solution. Herein, the Michael addition reaction was utilized to react with the double bond on the amphiphilic copolymers with the amino group of cystamine and, thus, to form three layers cross-linked polymer micelles. The poly(methacrylic acid) (PMAA) inner core of micelles was used to encapsulate hydrophobic anticancer drug doxorubicin (DOX) and realize the pH-responsiveness at tumor site. The cross-linked middle layer poly(2-hydroxyethyl methacrylate) (PHEMA) containing disulfide bond, not only could form the second cross-linked structure, but also could be used for reduction-responsiveness to release drug under high concentration of GSH. The outer hydrophilic block poly(poly(ethylene glycol) methyl ether methacrylate) (PPEGMA) shell was used for maintaining the stability of micelle structure (Scheme 1). The effects of different hydrophilic and hydrophobic block ratios of polymer micelles with the same hydrophilic and hydrophobic blocks used in the drug delivery system were studied, including systematic investigation the effects of different hydrophilic and hydrophobic block ratios on self-assembly, drug loading and release behavior of these polymer micelles.

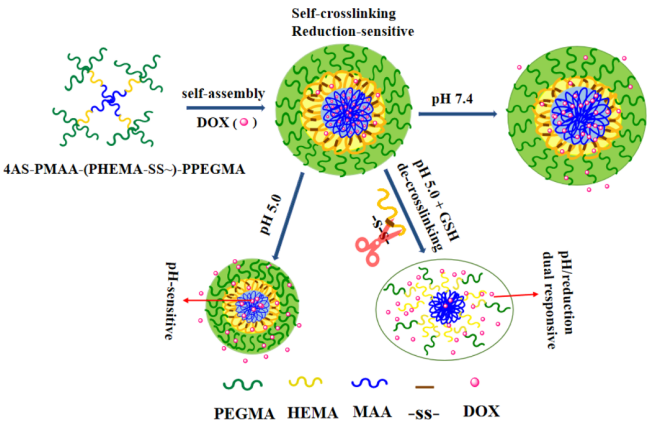

Scheme 1. Illustration of DOX-loaded and released from 4AS-PMAA-(PHEMA-SS~)-PPEGMA polymer micelles by pH/reduction triggered.

2. Experimental

2.1. Materials

Pentaerythritol (99%, Aldrich) was dried by vacuum distillation. Tertiary-butyl methacrylate (*t*BMA, TCI-EP), 2-hydroxyethyl methacrylate (HEMA, 99%, Aldrich), and poly(ethylene glycol) methyl ether methacrylate (PEGMA, M_n = 475 Da, 99%, Aldrich) were went through a neutral alumina column for purification before use. 2-bromoisobutyryl bromide (98%), 1,1,4,7,10,10-hexamethyltriethylenetetramine (HMTETA, 99%), methacryloyl chloride (95%), and triethylamine (TEA), all from J&K Scientific Ltd., were used as received. Doxorubicin hydrochloride (DOX·HCl) (Wuhan Yuancheng Gongchuang Technology Co., Ltd.), cystamine dihydrochloride (98%, Aldrich), trifluoroacetic acid (TFA), cupric bromide ($CuBr_2$), stannous octoate ($Sn(Oct)_2$), and other reagents were used directly.

2.2. Synthesis of copolymers

The four-arm star copolymers of 4AS-PMAA$_x$-(PHEMA-SS~)$_y$-PPEGMA$_z$ with different block ratios were synthesized through four steps (Scheme 2). First, the initiator pentaerythritol tetrakis (2-bromoisobutyrate) [Br_4] was prepared by treating pentaerythritol (5.45 g, 40 mmol) with 2-bromoisobutyryl bromide (19.78 mL, 160 mmol) in an ice/water bath for 5 h and then another 24 h at 25 °C. Yield: 89.7%. ^{1}H nuclear magnetic resonance (^{1}H NMR) (400 MHz, $CDCl_3$): Br_4: δ 1.93, 4.33. Second, with Br_4 as initiator and $CuBr_2$/HMTETA/$Sn(Oct)_2$ as catalyst system, four kinds of 4AS-P*t*BMA$_x$-(PHEMA)$_y$-PPEGMA$_z$ copolymers with different block ratios were synthesized by the ARGRT ATRP of the first monomer *t*BMA at 65 °C for 5 h, the second monomer HEMA at 55 °C for 12 h and third monomer PEGMA at 55 °C for 48 h under stirring by controlling the different feed ratio of monomers. Yield: 78.5%, 85.2%, 68.8% and 84.3%. ^{1}H NMR (400 MHz, $CDCl_3$): P*t*BMA: δ 0.8-1.2, 1.41, 1.62; PHEMA: δ 3.84, 4.09; PPEGMA: δ 3.38, 3.66, 4.30. M_n (^{1}H NMR) = 29.1, 46.8, 18.3, and 29.0 kg/mol.

Third, 4AS-P*t*BMA$_x$-(PHEMA-SS~)$_y$-PPEGMA$_z$ copolymers were reacted acylation reaction with TEA and methacryloyl chloride (shorten as A) in an ice/water bath for 2 h and at 25 °C for another 22 h, and then the obtained 4AS-P*t*BMA$_x$-(PHEMA-A)$_y$-PPEGMA$_z$ acylated copolymers were treated with cross-linker of cys-

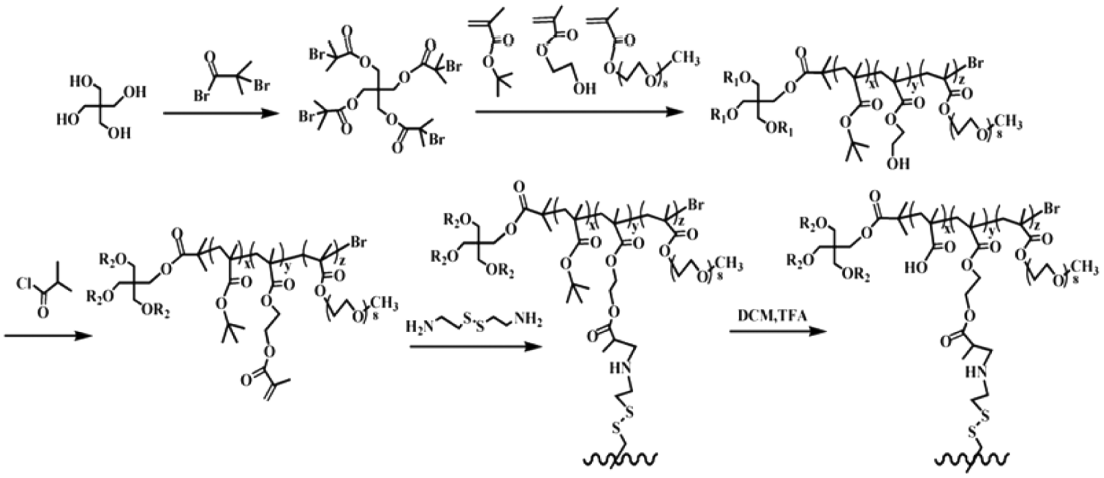

Scheme 2. Synthetic route of the star copolymer 4AS-PMAA$_x$-(PHEMA-SS~)$_y$-PPEGMA$_z$.

tamine dihydrochloride by dialysis in a PBS buffer solution (pH 9.0) with refreshing every 3 h for first 18 h and every 8 h for another 16 h. After these, the cross-linked products 4AS-PtBMA$_x$-(PHEMA-SS~)$_y$-PPEGMA$_z$ were received. Yield: 72.7%, 67.6%, 77.5% and 69.3%.^{1}H NMR (400 MHz, $CDCl_3$): PHEMA-A: δ 3.84, 4.09, 5.61, 6.16; PHEMA-SS~: δ 3.84, 4.09. Finally, 4AS-P*t*BMA$_x$-(PHEMA-SS~)$_y$-PPEGMA$_z$ copolymers were reacted with TFA in an ice/water bath for 30 min and at 25 °C for another 4 h, and then the final target copolymers 4AS-PMAA$_x$-(PHEMA-SS~)$_y$-PPEGMA$_z$ were obtained after removing all solvents and drying under vacuum overnight.[25,26] Yield: 86.8%, 85.4%, 83.2% and 81.6%. ^{1}H NMR (400 MHz, $CDCl_3$): PMAA: δ 0.8-1.2, 1.62, 12.30.

2.3. CMC measurement

The critical micelle concentration (CMC) value of copolymer was measured as following: The prepared pyrene/acetone solution (6.0×10^{-5} M) was placed into seventeen of volumetric bottles, and then added different concentrations of the polymer aqueous solution (0.0001~0.1 mg /mL) into each bottle after the acetone evaporated. With the final concentration of pyrene of 6.0×10^{-7} M, oscillated several times to make the solution uniform and balanced in the dark for 24 h. Then the fluorescence intensity was measured to obtain the CMC value on a fluorescence spectrometer (Hitachi F-7000).

2.4. Preparation of micelles

The 4AS-PMAA$_x$-(PHEMA-SS~)$_y$-PPEGMA$_z$ polymer (60 mg) was dissolved in DMSO (20 mL), and DOX solution (14 mg or 28 mg of DOX·HCl dissolved in 20 mL of DMSO) with its hydrochloride removed was added to the DMSO solution of the polymer, while DOX solution was not needed to be added to the blank micelles. Subsequently, micellar solution was received by dialysis method, and then filtered by 0.45 μm filter. After that, the blank and DOX-loaded micelles were obtained after freeze-drying. The particle size, zeta potential and morphology of the blank and DOX-loaded micelles were measured by dynamic light scattering (DLS) and transmission electron microscopy (TEM), and the drug loading content (DLC) and drug loading efficiency (DLE) of DOX-loaded micelles were obtained by UV absorption spectra.

2.5. *In vitro* DOX release

The *in vitro* controlled release of DOX was conducted in an incubation shaker (Shanghai Yiheng THZ-100) with a rotation speed of 100 rpm at 37 °C. DOX-loaded micelles (5 mg) with different polymer block ratios dissolved in 5 mL of three kinds of PBS buffer solutions ((1) pH 7.4, (2) pH 5.0, (3) pH 5.0 + 10 mM GSH)) were added into dialysis bags (MWCO = 3.5 kDa), and then the bags were transferred into 95 mL of corresponding buffer solutions and placed in the shaker. At the pre-determined time intervals, 4 mL of dialysate was taken out and measured on a fluorescence spectrometer (Hitachi F-7000) to get the released DOX concentration, and 4 mL of corresponding fresh buffer solution was added to keep the solution volume constant.

2.6. Measurements

Chemical structure of 4AS-PMAA$_x$-(PHEMA-SS~)$_y$-PPEGMA$_z$ and its precursors were characterized by ^{1}H NMR spectra (Bruker Avance III 400MHz NMR spectrometer), using deuterated chloroform ($CDCl_3$) or deuterated dimethyl sulfoxide (DMSO-d_6) as solvent. The structure of the synthesized polymers were measured by a Fourier transform infrared (FT-IR) spectrophotometer (Nicolet Nexus for Euro, USA) with the spectrum was obtained from 400 cm^{-1} to 4000 cm^{-1}. The number-average molecular weight (M_n) and polydispersity index (M_w/M_n) were measured by gel permeation chromatography (GPC) using an Agilent 1200 series GPC system using HPLC-grade THF as the mobile phase with a flow rate of 1.0 mL/min at 30 °C. Hydrodynamic diameter and zeta potential of the polymer micelles were analyzed by DLS (Brookhaven BI-200SM). Each sample was tested three times at a 632.8 nm He-Ne laser and the detection angle of 90° at 25 °C. Morphology of the polymer micelles was obtained by TEM (Tecnai G220 TEM). Drug-loading capacity was calculated from a UV-vis spectrophotometer (TU-1901) at 480 nm. CMC value and *in vitro* DOX release behavior were measured on a fluorescence spectrometer (Hitachi F-7000), with 350-420 nm of emission after excitation

at 340 nm and 480-720 nm of emission after excitation at 465 nm, respectively.

3. Results and discussion

3.1. Synthesis and characterization of 4AS-P*t*BMA$_x$-PHEMA$_y$-PPEGMA$_z$

The successful synthesis of 4AS-P*t*BMA$_x$-PHEMA$_y$-PPEGMA$_z$ was validated by ^{1}H NMR (Figure 1(A)) and FT-IR spectra (Figure 1(B)). In Figure 1(A), the characteristic peaks of P*t*BMA block appeared at δ 1.62 (c), 0.8-1.2 (d) and 1.4 (e) were due to the structure of -CH_2-, -CCH_3, and -$O(CH_3)_3$, respectively, and the chemical shifts at δ 3.84 (g) and δ 4.09 ppm (f) were ascribed to the structure of -CH_2CH_2- in the PHEMA block. Besides, the PPEGMA block displayed clear chemical shifts at δ 4.30 (h), 3.66 (i), and 3.38 ppm (j), owing to the structure of -COO-CH_2-, -OCH_2CH_2O-, and the end -OCH_3, respectively.

In Figure 1(B), the bands of 2933 and 2976 cm^{-1} were the stretching vibrations of -CH_3, while the bands of 2869 and 1460-1360 cm^{-1} corresponded to the stretching and bending vibrations of -CH_2- in the backbone. The bands of 1727 and 1148 cm^{-1} were the stretching vibrations of C=O and C-O in the carbonyl group of monomer units, and the stretching vibration of -OH for the PHEMA block appeared at the bands 3443 cm^{-1}. However, the characteristic band (1640 cm^{-1}) of C=C did not appear, indicating that the final copolymer product has been synthesized successfully.

According to the signals in ^{1}H NMR of 4AS-P*t*BMA$_x$-PHEMA$_y$-PPEGMA$_z$ (Figure 1(A)), the degree of polymerizations (DP) of P*t*BMA (x), PHEMA (y), PPEGMA (z), and the M_n were calculated (Table 1). Moreover, the four 4AS-P*t*BMA$_x$-PHEMA$_y$-PPEGMA$_z$ copolymers with different block ratios were also characterized by GPC (Figure 2), and the M_n and M_w/M_n were listed in Table 1. All the GPC traces were monomodal symmetric distribution, and the M_n were consistent with the values calculated on the base of ^{1}H NMR.

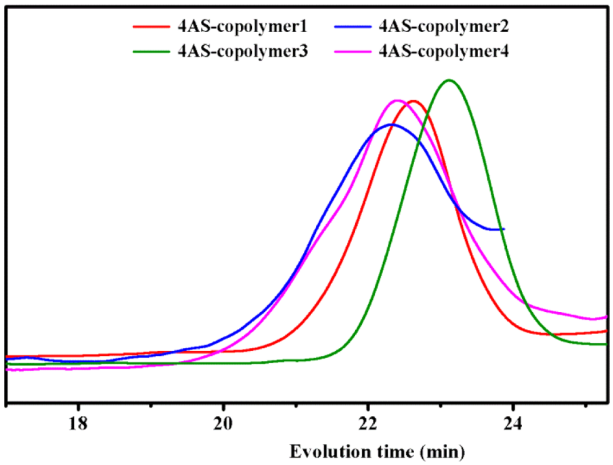

Figure 2. GPC traces of 4AS-P*t*BMA$_x$-(PHEMA-A)$_y$-PPEGMA$_z$.

We measured the critical micelle concentration (CMC) values of the four copolymers 4AS-P*t*BMA$_x$-PHEMA$_y$-PPEGMA$_z$ with different block ratios when these amphiphilic star copolymers self-assembled into three layers non-cross-linked micelles. As the fluorescence absorption peak of pyrene probe at 385.2 nm had a red shift to $I_{388.6}$ with the pyrene probe migrated from the

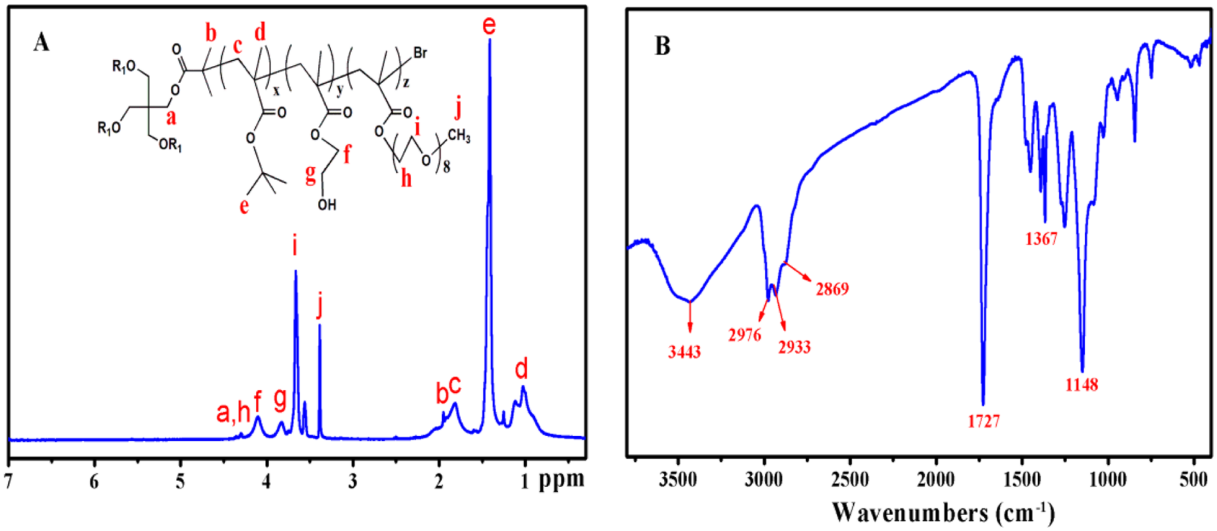

Figure 1. (A) ^{1}H NMR and (B) FT-IR spectra of 4AS-P*t*BMA$_x$-PHEMA$_y$-PPEGMA$_z$.

Table 1. ^{1}H NMR and GPC data of 4AS-P*t*BMA$_x$-PHEMA$_y$-PPEGMA$_z$

Copolymer	$M_{n,Th}$ [a]	x[b]	y[b]	z[b]	$M_{n,NMR}$ [c]	$M_{n,GPC}$ [d]	M_w/M_n [d]
4AS-copolymer 1	36,124	7.9	13.2	9.1	29,053	26,405	1.45
4AS-copolymer 2	51,828	9.9	17.1	16.8	46,847	34,605	1.54
4AS-copolymer 3	25,532	11.4	7.4	4.0	18,335	13,789	1.32
4AS-copolymer 4	33,244	21.2	13.1	5.1	28,956	26,078	2.09

[a] $M_{n,Th}$ and DP_{Th} calculated by theory. [b] DP_{NMR} calculated by the equations x = 2/3 × I_e/I_b, y = 9/2 × I_f/I_e × x, z = 2/3 × I_j/I_f × y, and $M_{n,NMR}$ = (142 × x + 130 × y + 475 × z) × 4 + 412 from ^{1}H NMR spectra. [c] $M_{n,NMR}$ calculated by the equation $M_{n,NMR}$ = (142 × x + 130 × y + 475 × z) × 4 + 412. [d] $M_{n,GPC}$ measured by GPC in THF.

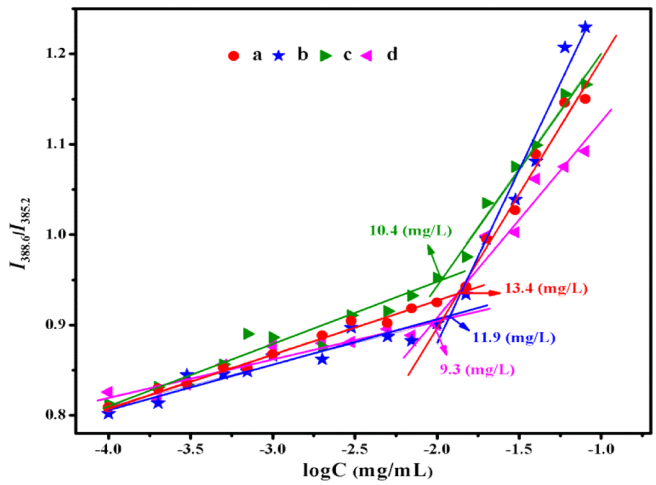

Figure 3. Plot of intensity ratios ($I_{388.6}/I_{385.2}$) as a function on the concentrations of copolymer (a) 4AS-P*t*BMA$_{7.9}$-PHEMA$_{13.2}$-PPEGMA$_{9.1}$, (b) 4AS-P*t*BMA$_{9.9}$-PHEMA$_{17.1}$-PPEGMA$_{16.8}$, (c) 4AS-P*t*BMA$_{11.4}$-PHEMA$_{7.4}$-PPEGMA$_{4.0}$, and (d) 4AS-P*t*BMA$_{21.2}$-PHEMA$_{13.1}$-PPEGMA$_{5.1}$.

aqueous solution into the inner core of micelles, the ratios of $I_{388.6}$ to $I_{385.2}$ against different polymer concentrations were obtained to get the CMC values at the interception of their two straight lines (Figure 3). The CMC values of 4AS-P*t*BMA$_{7.9}$-PHEMA$_{13.2}$-PPEGMA$_{9.1}$, 4AS-P*t*BMA$_{9.9}$-PHEMA$_{17.1}$-PPEGMA$_{16.8}$, 4AS-P*t*BMA$_{11.4}$-PHEMA$_{7.4}$-PPEGMA$_{4.0}$, and 4AS-P*t*BMA$_{21.2}$-PHEMA$_{13.1}$-PPEGMA$_{5.1}$ were 13.4, 11.9, 10.4, and 9.3 mg/L, respectively, decreasing with the increase of the length of P*t*BMA. For example, the CMC of 4AS-P*t*BMA$_{21.2}$-PHEMA$_{13.1}$-PPEGMA$_{5.1}$ (9.3 mg/mL) was lower than 4AS-P*t*BMA$_{7.9}$-PHEMA$_{13.2}$-PPEGMA$_{9.1}$ (13.4 mg/mL). The CMC values of the copolymers 4AS-P*t*BMA$_x$-PHEMA$_y$-PPEGMA$_z$ with different block ratios were much lower than those of general surfactants, which were beneficial for the polymer micelles to maintain good stability even at lower concentrations.[27]

3.2. Synthesis and characterization of 4AS-PMAA$_x$-(PHEMA-SS~)$_y$-PPEGMA$_z$

The successful synthesis of copolymer 4AS-PMAA$_x$-(PHEMA-SS~)$_y$-PPEGMA$_z$ and its precursors were characterized by ^{1}H NMR

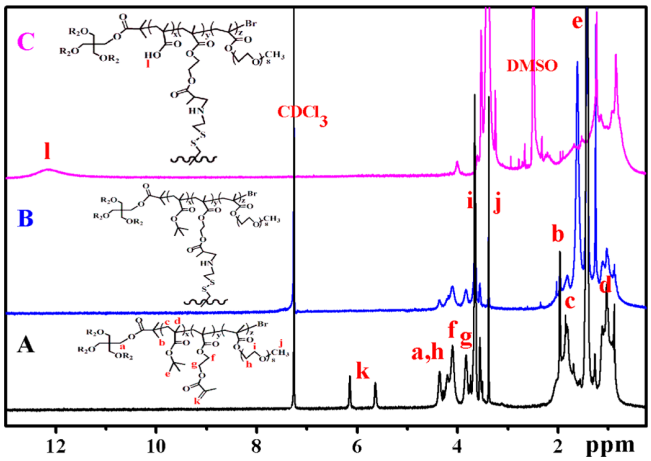

Figure 4. ^{1}H NMR spectra of (A) 4AS-P*t*BMA$_x$-(PHEMA-A)$_y$-PPEGMA$_z$ and (B) 4AS-P*t*BMA$_x$-(PHEMA-SS~)$_y$-PPEGMA$_z$ in CDCl$_3$, and (C) 4AS-PMAA$_x$-(PHEMA-SS~)$_y$-PPEGMA$_z$ in DMSO.

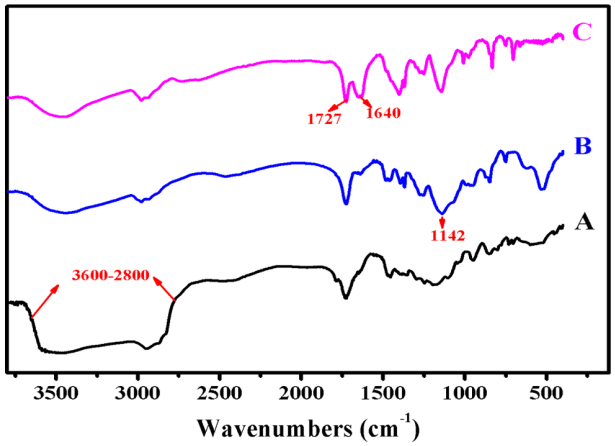

Figure 5. FT-IR spectra of (A) 4AS-P*t*BMA$_x$-(PHEMA-A)$_y$-PPEGMA$_z$, (B) 4AS-P*t*BMA$_x$-(PHEMA-SS~)$_y$-PPEGMA$_z$, and (C) 4AS-PMAA$_x$-(PHEMA-SS~)$_y$-PPEGMA$_z$.

(Figure 4) and FT-IR spectra (Figure 5). ^{1}H NMR of 4AS-P*t*BMA$_x$-(PHEMA-A)$_y$-PPEGMA$_z$ revealed that signals at δ 5.61 and 6.16 attributable to the C=C group appeared (Figure 4(A)). The FT-IR spectrum of 4AS-P*t*BMA$_x$-(PHEMA-A)$_y$-PPEGMA$_z$ had an intense band of the C=C group at 1640 cm^{-1} (Figure 5(A)) compared to the spectrum of 4AS-P*t*BMA$_x$-PHEMA$_y$-PPEGMA$_z$ (Figure 1(B)). However, after crosslinking, the band at 1640 cm^{-1} disappeared and changes in the ~1142 cm^{-1} area characteristic of bands were assigned to C-N groups (Figure 5(B)). ^{1}H NMR and FT-IR spectra indicated that the formation of crosslinking structure. As to the ^{1}H NMR of 4AS-PMAA$_x$-(PHEMA-SS~)$_y$-PPEGMA$_z$, the characteristic -COOH signals of PMAA at δ 12.30 were clearly observed while the -C(CH$_3$)$_3$ signals of P*t*BMA at δ 1.41 disappeared (Figure 4(C)). And, the FT-IR spectrum of 4AS-PMAA$_x$-(PHEMA-SS~)$_y$-PPEGMA$_z$ exhibited a larger broad shoulder at 2800-3600 cm^{-1} for the stretching vibration of -COOH group of PMAA (Figure 5(C)). Thus, all these data demonstrated that the final products 4AS-PMAA$_x$-(PHEMA-SS~)$_y$-PPEGMA$_z$ had been synthesized successfully.

The obtained copolymers 4AS-PMAA$_x$-(PHEMA-SS~)$_y$-PPEGMA$_z$ with different block ratios self-assembled into three layers cross-linked micelles in aqueous solution when the concentration reached their CMC values, and the measured results were shown in Figure 6. The CMC values of 4AS-PMAA$_{7.9}$-(PHEMA-SS~)$_{13.2}$-PPEGMA$_{9.1}$, 4AS-PMAA$_{9.9}$-(PHEMA-SS~)$_{17.1}$-PPEGMA$_{16.8}$, 4AS-PMAA$_{11.4}$-(PHEMA-SS~)$_{7.4}$-PPEGMA$_{4.0}$ and 4AS-PMAA$_{21.2}$-(PHEMA-SS~)$_{13.1}$-PPEGMA$_{5.1}$ were 4.6, 3.9, 3.4, and 1.9 mg/L, respectively. Compared with non-cross-linked micelles self-assembled by the copolymer 4AS-P*t*BMA$_x$-PHEMA$_y$-PPEGMA$_z$, these cross-linked micelles had lower CMC values, indicating that the cross-linked micelles owned better stability than non-cross-linked micelles.

3.3. Characterization of the blank and DOX-loaded cross-linked micelles

The blank and DOX-loaded 4AS-PMAA$_x$-(PHEMA-SS~)$_y$-PPEGMA$_z$ micelles with different block ratios were prepared by dialysis method, and their physico-chemical properties, such as particle

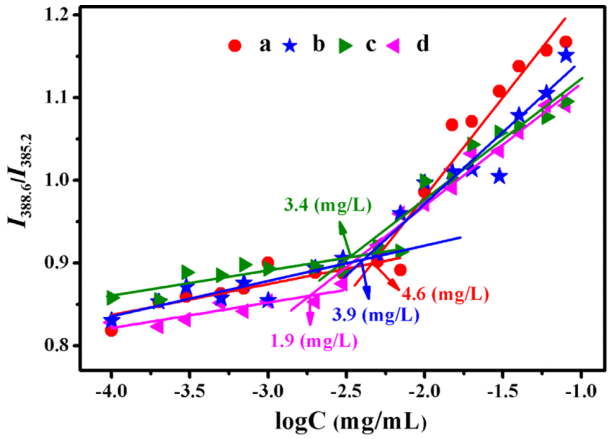

Figure 6. Plot of intensity ratios ($I_{388.6}/I_{385.2}$) as a function on the concentrations of copolymer (a) 4AS-PMAA$_{7.9}$-(PHEMA-SS~)$_{13.2}$-PPEGMA$_{9.1}$, (b) 4AS-PMAA$_{9.9}$-(PHEMA-SS~)$_{17.1}$-PPEGMA$_{16.8}$, (c) 4AS-PMAA$_{11.4}$-(PHEMA-SS~)$_{7.4}$-PPEGMA$_{4.0}$, and (d) 4AS-PMAA$_{21.2}$-(PHEMA-SS~)$_{13.1}$-PPEGMA$_{5.1}$.

size, zeta potential, DLC and DLE were shown in Table 2. The feed ratios of DOX to polymer have very important influence on DLC and DLE, and the DLC increased with the increase of the ratio. As the hydrophobic anticancer drug DOX was mainly loaded onto the hydrophobic PMAA core through electrostatic interaction, the longer of PMAA core and hydrophobic PHEMA cross-linked middle layer triggered the larger amounts of DOX encapsulated into micelles which resulted in the increased DLC. For example, at the feed ratio 14/60 (DOX/polymer, mg/mg), the DLC of 4AS-PMAA$_{7.9}$-(PHEMA-SS~)$_{13.2}$-PPEGMA$_{9.1}$, 4AS-PMAA$_{11.4}$-(PHEMA-SS~)$_{7.4}$-PPEGMA$_{4.0}$, and 4AS-PMAA$_{21.2}$-(PHEMA-SS~)$_{13.1}$-PPEGMA$_{5.1}$ were increased in turn, the values of which were 14.33%, 15.33%, and 16.57%. Owning to the limited solubilization capacity of the inner core of polymer micelles to DOX, the DLE would decrease when continued increased the feed ratio.

After DOX-loading, the particle size of micelles increased compared with those of the blank micelles, indicating that DOX was incorporated into the micelles through electrostatic interaction effectively. The particle size of cross-linked micelles increased apprently with the increasing molecular weight and length of PMAA core and hydrophobic PHEMA cross-linked middle layer, which could be seen in Table 2 that the particle size of 4AS-PMAA$_{21.2}$-(PHEMA-SS~)$_{13.1}$-PPEGMA$_{5.1}$ micelles was much larger than that of 4AS-PMAA$_{11.4}$-(PHEMA-SS~)$_{7.4}$-PPEGMA$_{4.0}$ micelles. The size distributions of blank and DOX-loaded micelles were both small, indicating that the polymer micelles had good dispersion. Although the brush-like PPEGMA block in micellar shell had a strong shielding effect on PMAA core, the carboxylic groups in PMAA segments had a protonation in aqueous solution at pH > 5, leading to the negative charges of micelles. The 4AS-PMAA$_{21.2}$-(PHEMA-SS~)$_{13.1}$-PPEGMA$_{5.1}$ micelles with the longest negatively charged PMAA core had lowest zeta potential.

The TEM images of 4AS-PMAA$_{11.4}$-(PHEMA-SS~)$_{7.4}$-PPEGMA$_{4.0}$ blank and DOX-loaded micelles were shown in Figure 7, which were owned spherical morphology. The size of blank micelles was about 100 nm whlie the DOX-loaded micelles had a bigger size which around 150 nm, and these results were in agreement with those determined by DLS.

3.4. Effect of pH and GSH on the particle sizes of DOX-loaded micelles

Particle sizes of the DOX-loaded micelles with different polymer block ratios were measured at different stimulated condition. When the pH value was 7.4 (Figure 8(A)), the -COOH group in PMAA core changed to -COO- form and the electrostatic repulsion between -COO- caused the micelles to swell, leading to an increase in the micellar particle size and a wider size distribution after 24 h. After the pH value decreased to 5.0 (Figure 8(B)), the carboxyl group changed to the non-ionic form of -COOH, the electrostatic interaction between DOX and micelles was weakened, resulting in a decrease in the micellar particle size and a narrower size distribution after 24 h.[28,29] Among the four different block ratios of the DOX-loaded polymer micelles, polymer micelles of 4AS-PMAA$_{11.4}$-(PHEMA-SS~)$_{7.4}$-PPEGMA$_{4.0}$ and 4AS-PMAA$_{21.2}$-(PHEMA-SS~)$_{13.1}$-PPEGMA$_{5.1}$ contained more pH-responsive PMAA blocks and shorter hydrophilic PPEGMA blocks had smaller particle sizes. At pH 5.0 with 10 mM of GSH condition (Figure 8(C)), the micellar particle sizes were further decreased. As the polymer micelles of 4AS-PMAA$_{11.4}$-(PHEMA-SS~)$_{7.4}$-PPEGMA$_{4.0}$ contained the smallest cross-linked layer block, the micellar particle size changed to a bimodal distribution with a wide distribution of more than 1,000 nm after 24 h, indicating that the

Table 2. D_h, PDI, zeta potential, DLC and DLE of blank and DOX-loaded cross-linked micelles

Sample	DOX/polymer (mg/mg)	DLC (%)	DLE (%)	D_h (nm)	PDI	Zeta potential (mV)
4AS-PMAA$_{7.9}$-(PHEMA-SS~)$_{13.2}$-PPEGMA$_{9.1}$	0/60			163.8	0.216	-15.87
	14/60	14.33	71.70	198.6	0.279	-14.41
	28/60	22.81	63.33	213.5	0.234	-12.35
4AS-PMAA$_{9.9}$-(PHEMA-SS~)$_{17.1}$-PPEGMA$_{16.8}$	0/60			172.5	0.288	-21.49
	14/60	14.73	74.05	208.6	0.385	-19.88
	28/60	24.29	68.76	231.9	0.279	-20.39
4AS-PMAA$_{11.4}$-(PHEMA-SS~)$_{7.4}$-PPEGMA$_{4.0}$	0/60			127.5	0.190	-23.07
	14/60	15.33	77.61	170.6	0.153	-21.98
	28/60	25.01	71.47	175.0	0.217	-22.35
4AS-PMAA$_{21.2}$-(PHEMA-SS~)$_{13.1}$-PPEGMA$_{5.1}$	0/60			162.3	0.152	-30.50
	14/60	16.57	85.13	190.2	0.211	-27.13
	28/60	27.97	83.22	195.5	0.213	-34.01

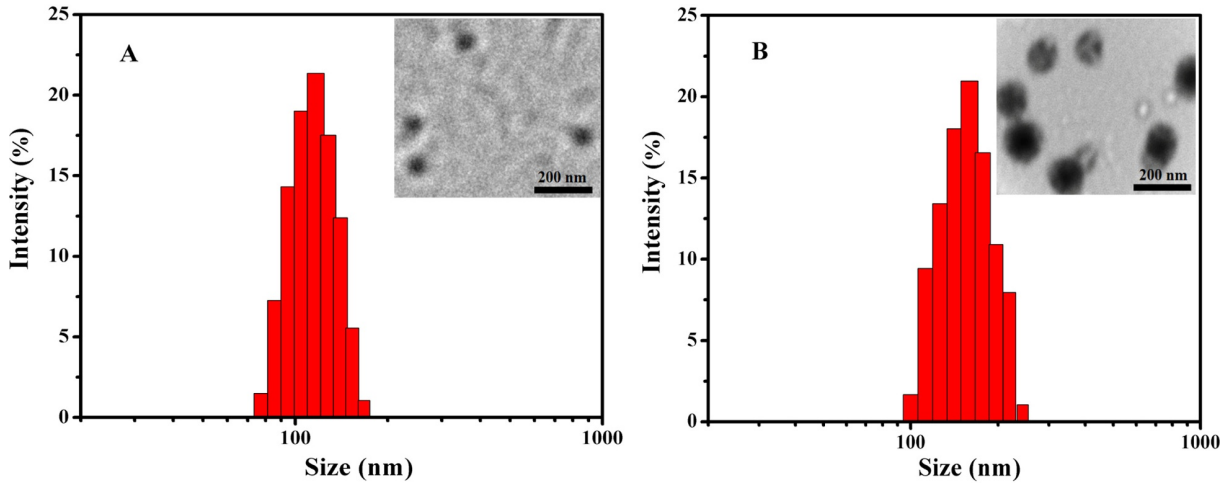

Figure 7. DLS and TEM of (A) blank and (B) DOX-loaded 4AS-PMAA$_{11.4}$-(PHEMA-SS~)$_{7.4}$-PPEGMA$_{4.0}$ micelles.

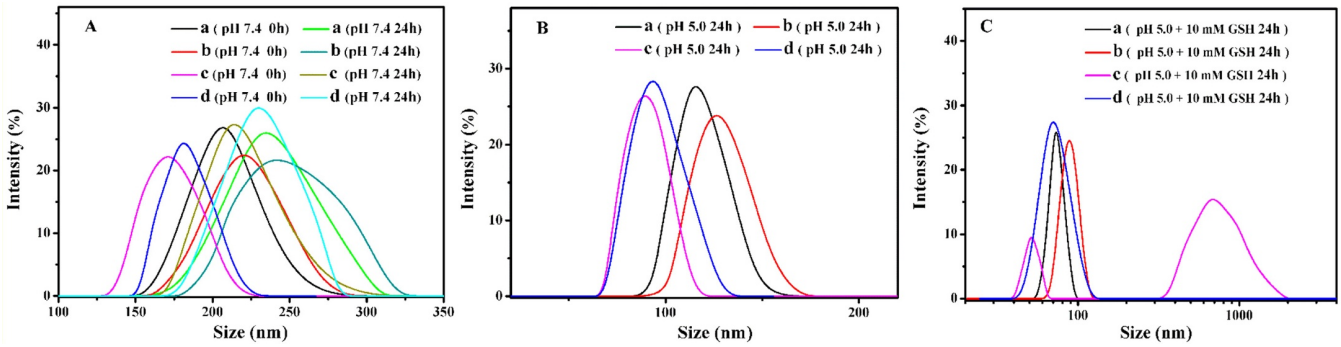

Figure 8. The changes in particle sizes of the DOX-loaded micelles (the feed ratio of DOX/polymer = 28/60) with different polymer block ratios: (a) 4AS-PMAA$_{7.9}$-(PHEMA-SS~)$_{13.2}$-PPEGMA$_{9.1}$, (b) 4AS-PMAA$_{9.9}$-(PHEMA-SS~)$_{17.1}$-PPEGMA$_{16.8}$, (c) 4AS-PMAA$_{11.4}$-(PHEMA-SS~)$_{7.4}$-PPEGMA$_{4.0}$, and (d) 4AS-PMAA$_{21.2}$-(PHEMA-SS~)$_{13.1}$-PPEGMA$_{5.1}$ dispersed in pH 6.9 deionized water at different stimulated condition of (A) pH 7.4, (B) pH 5.0, and (C) pH 5.0 + 10 mM GSH.

cross-linked structure was destroyed and the micellar architecture was disassembled to smaller units, and then the smaller units caused further obvious aggregations.

3.5. *In vitro* release of DOX

In order to evaluate the drug release performance of the polymer micelles with different block ratios, the *in vitro* release of DOX was studied under different conditions, *i.e.*, pH 7.4, pH 5.0 and pH 5.0 + 10 mM GSH.

Under the normal physiological condition of pH 7.4 (Figure 9(A)), The four DOX-loaded micelles were released slowly, only 11-25% of DOX at 7 h, and then the release rate basically kept constant with still only 18-37% of the DOX cumulative release percentages after 110 h. There had no sudden release phenomenon, indicating that the polymer micelles had good stability and strong resistance to dilute solution. The 4AS-PMAA$_{9.9}$-(PHEMA-SS~)$_{17.1}$-PPEGMA$_{16.8}$ micelles, owned to the longest cross-linked layer of PHEMA segments, had the lowest DOX cumulative release, indicating that the cross-linked structure acted as a barrier for drug release and inhibited the premature release of DOX effectively. As for the 4AS-PMAA$_{21.2}$-(PHEMA-SS~)$_{13.1}$-PPEGMA$_{5.1}$ micelles, the PMAA core were longest and the DOX cumulative release was the maximum.

When the pH decreased to weak acid of pH 5.0 (Figure 9(B)), 42-56% of DOX was released at 3 h, and the DOX cumulative release percentages reached to 70-84% after 110 h. Under this acidic condition, the electrostatic interaction between DOX and micelles was weakened and PMAA core induced the shrink of the micelles, leading to the higher cumulative release.[28,29] With the longer of PMAA block, the responsiveness of micellar core to pH stimulation was enhanced, and the 4AS-PMAA$_{21.2}$-(PHEMA-SS~)$_{13.1}$-PPEGMA$_{5.1}$ micelles had a higher DOX cumulative release percentage than those of other micelles.

After the introduction of 10 mM GSH (Figure 9(C)), the DOX cumulative release percentages in tumor cells (pH 5.0+ 10 mM GSH) reached to 53-57% at 2 h and 83-90% after 110 h. Under this condition, On the one hand, the PMAA was in response to the pH stimulation with improving the DOX release. On the other hand, with the broken of disulfide bonds in the cross-linked micelles at the reductive environment of 10 mM GSH, the cross-linked structures were destroyed, resulting in the rapid release of DOX. In the polymer micelles with different block ratios, the 4AS-PMAA$_{21.2}$-(PHEMA-SS~)$_{13.1}$-PPEGMA$_{5.1}$ micelles, owned the longest PMAA core had the highest cumulative release of 90.1%. However, compared with the release without GSH, as the PHEMA cross-linked middle layer were longest in the 4AS-PMAA$_{9.9}$-(PHEMA-SS~)$_{17.1}$-PPEGMA$_{16.8}$ micelles, the DOX cumulative release increased

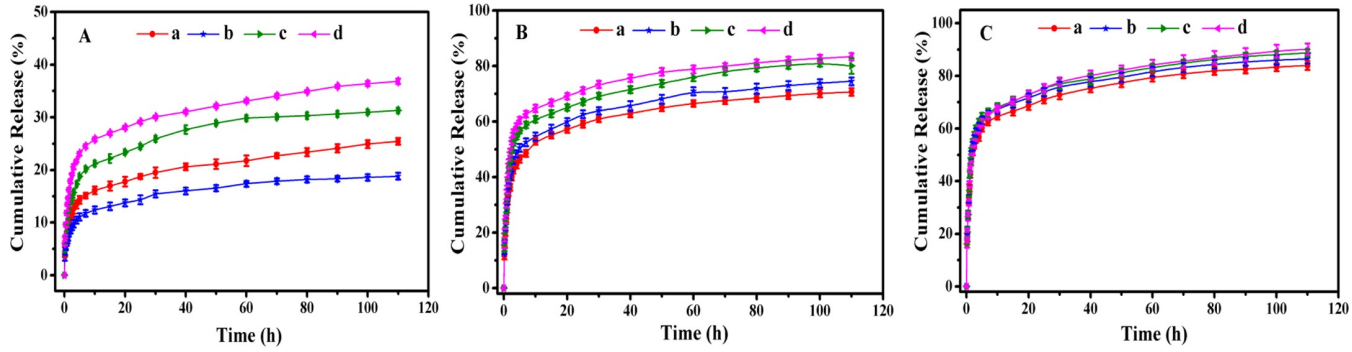

Figure 9. *In vitro* DOX release profiles of DOX-loaded polymer micelles of (a) 4AS-PMAA$_{7.9}$-(PHEMA-SS~)$_{13.2}$-PPEGMA$_{9.1}$, (b) 4AS-PMAA$_{9.9}$-(PHEMA-SS~)$_{17.1}$-PPEGMA$_{16.8}$, (c) 4AS-PMAA$_{11.4}$-(PHEMA-SS~)$_{7.4}$-PPEGMA$_{4.0}$ and (d) 4AS-PMAA$_{21.2}$-(PHEMA-SS~)$_{13.1}$-PPEGMA$_{5.1}$, at different simulated conditions of (A) pH 7.4, (B) pH 5.0, and (C) pH 5.0 + 10 mM GSH.

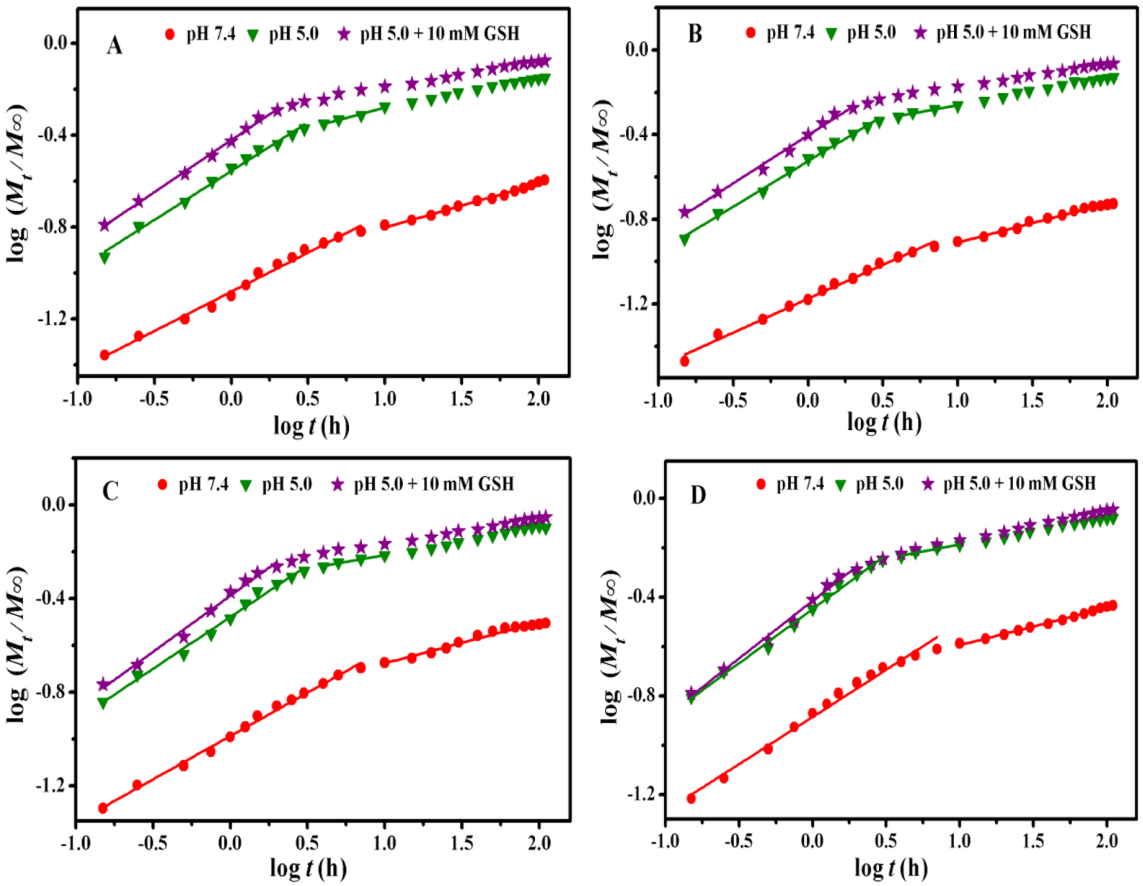

Figure 10. Plots of log (M_t/M_∞) *vs.* log *t* for DOX release from DOX-loaded polymer micelles of (A) 4AS-PMAA$_{7.9}$-(PHEMA-SS~)$_{13.2}$-PPEGMA$_{9.1}$, (B) 4AS-PMAA$_{9.9}$-(PHEMA-SS~)$_{17.1}$-PPEGMA$_{16.8}$, (C) 4AS-PMAA$_{11.4}$-(PHEMA-SS~)$_{7.4}$-PPEGMA$_{4.0}$, and (D) 4AS-PMAA$_{21.2}$-(PHEMA-SS~)$_{13.1}$-PPEGMA$_{5.1}$ under different simulated conditions of pH 7.4, pH 5.0 and pH 5.0 + 10 mM GSH.

the most after introducing 10 mM of GSH.

The DOX release mechanisms of these four kinds of micelles with different block ratios were studied using the following semi-empirical equation established by Ritger and Peppas.[30-32]

$$\log\left(\frac{M_t}{M_\infty}\right) = n\log t + \log k \quad (1)$$

where M_t and M_∞ represent the cumulative drug release at time t and infinite time, respectively, k is a constant incorporating the structural and geometric characteristics of the polymer matrix and n is the release exponent indicating the drug release mechanism. The obtained parameters were shown in Figure 10 and summarized in Table 3.

As for the four DOX-loaded cross-linked micelles, all correlation coefficient R^2 of above 0.9 were relatively ideal. The n values of stage I and stage II were all less than 0.43 at pH 7.4, suggesting all the release processes were mainly for diffusion and erosion control. That was because the cross-linked structure made the micelles had a strong ability to resist dilute solution and maintain stability. In this condition, the 4AS-PMAA$_{9.9}$-(PHEMA-SS~)$_{17.1}$-PPEGMA$_{16.8}$ micelles, owned the longest hydrophobic PHEMA cross-linked middle layer and relatively longer of hydro-

Table 3. Fitting parameters of the *in vitro* DOX release mechanism at different conditions of pH 7.4, pH 5.0 and pH 5.0 + 10 mM GSH

Micelles	Condition	n_1	k_1	R_1^2	n_2	k_2	R_2^2
4-AS-PMAA$_{7.9}$-SS-PHEMA$_{13.2}$-PPEGMA$_{9.1}$	pH 7.4[a]	0.3412	0.0829	0.9904	0.1914	0.1015	0.9917
	pH 5.0[b]	0.4250	0.2780	0.9923	--	--	--
	pH 5.0 + 10 mM GSH[c]	0.4521	0.3792	0.9966	--	--	--
4-AS-PMAA$_{9.9}$-SS-PHEMA$_{17.1}$-PPEGMA$_{16.8}$	pH 7.4[a]	0.3209	0.0668	0.9911	0.1839	0.0806	0.9894
	pH 5.0[b]	0.4293	0.2985	0.9956	--	--	--
	pH 5.0 + 10 mM GSH[c]	0.4546	0.3961	0.9919	--	--	--
4-AS-PMAA$_{11.4}$-SS-PHEMA$_{7.4}$-PPEGMA$_{4.0}$	pH 7.4[a]	0.3699	0.1033	0.9947	0.1755	0.1409	0.9755
	pH 5.0[b]	0.4413	0.3327	0.9910	--	--	--
	pH 5.0 + 10 mM GSH[c]	0.4784	0.4101	0.9898	--	--	--
4-AS-PMAA$_{21.2}$-SS-PHEMA$_{13.1}$-PPEGMA$_{5.1}$	pH 7.4[a]	0.3822	0.1302	0.9865	0.1613	0.1791	0.9948
	pH 5.0[b]	0.4388	0.3559	0.9949	--	--	--
	pH 5.0 + 10 mM GSH[c]	0.4667	0.3847	0.9913	--	--	--

[a]Stage I is 0-7 h, stage II is 7-110 h. [b]Stage I is 0-3 h, stage II is 3-10 h. [c]Stage I is 0-2 h.

philic stability PPEGMA outer shell to prevent the release of DOX, had the lowest k value than those of the other three micelles. In the cases of pH 5.0, the *n* values in stage I were all close to 0.43, indicating the DOX release was Fickian diffusion in the first 3 h. Under this acidic condition, the carboxylic acid group in PMAA core existed in non-ionic form, which induced the shrink of molecular chains. When went to the stage II, the DOX release behavior was similar to the behavior of pH 7.4, suggesting the release was changed to diffusion and erosion control. At pH 5.0 with 10 mM GSH, the n values of the four polymer micelles in stage I were all greater than 0.43 and less than 0.85. In the condition, cross-linked micelles not only had shrunk in response to the stimulation of pH, but also were destroyed the structures, so the DOX release behavior was owing to the anomalous transport mechanism. As the semi-empirical model was just suitable for less than 60% of the cumulative drug release, the cumulative drug releases were more than 60% in the 10-110 h stage at pH 5.0 and in the 3-110 h stage at pH 5.0 with 10 mM GSH, therefore, the n and k values were not calculated for these conditions.[33] Meanwhile, the *k* values of second stage were higher than those of first stage under all conditions, suggesting the DOX release rate accelerated with time. The 4AS-PMAA$_{11.4}$-(PHEMA-SS~)$_{7.4}$-PPEGMA$_{4.0}$ micelles owned the shortest of hydrophobic PHEMA cross-linked middle layer and relatively longer of pH responsive PMAA core had the highest of *k* value at pH 5.0 with 10 mM GSH condition, indicating the faster DOX release rate than other three micelles in all the conditions.

4. Conclusions

The four-arm star copolymers 4AS-PMAA$_x$-(PHEMA-SS~)$_y$-PPEGMA$_z$ with the same hydrophilic and hydrophobic blocks and different block ratios were designed and synthesized using the combination of continuous ARGET ATRP, Michael addition reaction and hydrolysis. The molecular weight and structures of these copolymers were confirmed by GPC, ^{1}H NMR and FT-IR spectra. The CMC values for these copolymers self-assembled into micelles were very low and decreased with the increase of the length of PMAA core and PHEMA cross-linked middle layer. The longer of PMAA core and HEMA cross-linked middle layer not only improved the DLC but also caused relatively bigger particle sizes of micelles. In the normal physiological condition (pH 7.4), the DOX-loaded cross-linked polymer micelles with different polymer block ratios showed good stability with low DOX released. Under the condition of tumor cell (pH 5.0 + 10 mM GSH), the cross-linked structure of micelles were destroyed along with fast release of DOX. The 4AS-PMAA$_{21.2}$-(PHEMA-SS~)$_{13.1}$-PPEGMA$_{5.1}$ micelles with the longest PMAA core had the largest cumulative release of 90.1% at tumor site. However, after the cross-linked structures were destroyed by introducing 10 mM of GSH, the 4AS-PMAA$_{11.4}$-(PHEMA-SS~)$_{7.4}$-PPEGMA$_{4.0}$ micelles owned the shortest of PHEMA layer had a faster DOX release rate than other three micelles at stage I. Therefore, the 4AS-PMAA$_x$-(PHEMA-SS~)$_y$-PPEGMA$_z$ polymer micelles can be used as a good carrier of hydrophobic anticancer drugs by optimization of the polymer structures and provide some basis for the design of stimuli-responsive cross-linked micelles.

References

(1) A. N. Lukyanov and V. P. Torchilin, *Adv. Drug Deliv. Rev.*, **56**, 1273 (2004).
(2) C. Sun, X. Li, X. Du, and T. Wang, *Int. J. Biol. Macromol.*, **112**, 65 (2018).
(3) L. Xiao, L. Huang, F. Moingeon, M. Gauthier, and G. Yang, *Biomacromolecules*, **18**, 2711 (2017).
(4) Y. Deng, H. Yuan, and W. Yuan, *J. Mater. Chem. B*, **7**, 286 (2019).
(5) Y. Q. Yang, W. J. Lin, L. J. Zhang, C. Z. Cai, W. Jiang, X. D. Guo, and Y. Qian, *Macromol. Res.*, **21**, 1011 (2013).
(6) D. Xiong, N. Yao, H. Gu, J. Wang, and L. Zhang, *Polymer*, **114**, 161 (2017).
(7) B. Pandey, N. G. Patil, G. S. Bhosle, A. V. Ambade, and S. S. Gupta, *Bioconjugate Chem.*, **30**, 633 (2019).
(8) Q. Chen, F. Han, C. Lin, X. Wen, and P. Zhao, *Polymer*, **146**, 378 (2018).
(9) T. Sim, S. M. Han, C. Lim, W. R. Won, E. S. Lee, Y. S. Youn, and K. T. Oh, *Macromol. Res.*, **27**, 795 (2019).
(10) N. Wang, X.-C. Chen, R.-L. Ding, X.-L. Yang, J. Li, X.-Q. Yu, K. Li, and X. Wei, *RSC Adv.*, **9**, 2371 (2019).
(11) X. Ma, J. Liu, L. Lei, H. Yang, and Z. Lei, *J. Appl. Polym. Sci.*, **136**, 47946 (2019).
(12) Z. Zhou, G. Li, N. Wang, F. Guo, L. Guo, and X. Liu, *Colloid. Surface. B*, **172**, 136 (2018).
(13) Z. Su, Y. Xu, Y. Wang, W. Shi, S. Han, and X. Shuai, *Biomater. Sci.*, **7**, 3821 (2019).

(14) X. Shan, J. Mao, M. Long, K. S. Ahmed, C. Sun, L. Qiu, and J. Chen, *J. Appl. Polym. Sci.*, **136**, 47854 (2019).
(15) Y. Li, K. Xiao, W. Zhu, W. Deng, and K. S. Lam, *Adv. Drug Deliv. Rev.*, **66**, 58 (2014).
(16) S. Mura, J. Nicolas, and P. Couvreur, *Nat. Mater.*, **12**, 991 (2013).
(17) L. Bu, H. Zhang, K. Xu, B. Du, C. Zhu, and Y. Li, *Drug Deliv.*, **26**, 300 (2019).
(18) L. Li, D. Li, M. Zhang, J. He, J. Liu, and P. Ni, *Bioconjugate Chem.*, **29**, 2806 (2018).
(19) Y. Qu, B. Chu, X. Wei, M. Lei, D. Hu, R. Zha, L. Zhong, M. Wang, F. Wang, and Z. Qian, *J. Control. Release*, **296**, 93 (2019).
(20) X. Sang, Q. Yang, G. Shi, L. Zhang, D. Wang, and C. Ni, *Mater. Sci. Engi. C*, **91**, 727 (2018).
(21) Z. Guo, K. Zhao, R. Liu, X. Guo, B. He, J. Yan, and J. Ren, *J. Mater. Chem. B*, **7**, 334 (2019).
(22) B. Ma, W. Zhuang, Y. Wang, R. Luo, and Y. Wang, *Acta Biomater.*, **70**, 186 (2018).
(23) Z. Zhang, Q. Qu, J. Li, and S. Zhou, *Macromol. Biosci.*, **13**, 789 (2013).
(24) Y. Q. Yang, B. Zhao, Z. D. Li, W. J. Lin, C. Y. Zhang, X. D. Guo, J. F. Wang, and L. J. Zhang, *Acta Biomater.*, **9**, 7679 (2013).
(25) Y. Q. Yang, W. J. Lin, B. Zhao, X. F. Wen, X. D. Guo, and L. J. Zhang, *Langmuir*, **28**, 8251 (2012).
(26) Y. Q. Yang, X. D. Guo, W. J. Lin, L. J. Zhang, C. Y. Zhang, and Y. Qian, *Soft Matter*, **8**, 454 (2012).
(27) Y.-N. Xue, Z.-Z. Huang, J.-T. Zhang, M. Liu, M. Zhang, S.-W. Huang, and R.-X. Zhuo, *Polymer*, **50**, 3706 (2009).
(28) J. Zeng, P. Du, L. Liu, J. Li, K. Tian, X. Jia, X. Zhao, and P. Liu, *Mol. Pharm.*, **12**, 4188 (2015).
(29) Tian, X. Jia, X. Zhao, and P. Liu, *Mol. Pharm.*, **13**, 2683 (2016).
(30) P. L. Ritger and N. A. Peppas, *J. Control. Release*, **5**, 23 (1987).
(31) J. Siepmann and N. A. Peppas, *Adv. Drug Deliv. Rev.*, **64**, 163 (2012).
(32) W. Lin, S. Nie, Q. Zhong, Y. Yang, C. Cai, J. Wang, and L. Zhang, *J. Mater. Chem. B*, **2**, 4008 (2014).
(33) P. L. Ritger and N. A. Peppas, *J. Control. Release*, **5**, 37 (1987).

